

Supporting Information:

Controlled perturbation of the thermodynamic equilibrium by microfluidic separation of porphyrin-based aggregates in a multi-component self-assembling system

Floris Helmich and E.W. Meijer.

Laboratory for Macromolecular and Organic Chemistry, Eindhoven University of Technology, P. O. Box 513, 5600 MB Eindhoven, the Netherlands.

Materials and Methods

The methylcyclohexane (MCH, Sigma-Aldrich) used in all experiments was spectroscopic grade. Deuterated MCH for DOSY analyses (Cambridge Isotope Laboratories) was provided with TMS as a 0 ppm reference. The synthetic procedure for **S-Zn** and **S-Zn-Me** is described in earlier work.^{S1}

Circular dichroism (CD) spectra were measured using a Jasco J-815 CD spectrometer, with temperature controlled by a PTC-348WI Peltier system. Ultraviolet-visible (UV-vis) absorbance spectra were recorded on and a Jasco V-650 UV-vis spectrometer with a Jasco ETCT-762 temperature controller. DOSY-NMR spectra were recorded on a Varian 500 MHz instrument.

For the microfluidic setup (Fig. S1A), stainless steel syringes (KDS, 2.5 ml with 1/16" Swagelok) were placed on a syringe pump (neMESYS starter and double module, 14.1 gearing). Via a 3-way HPLC switching valve (Rheodyne 7030), both stainless steel syringes were filled by 5 ml glass syringes (Fortuna optima with Luer lock) in one position and connected to the microfluidic chip in the other position. Via fused silica tubing (Upchurch Scientific, 360 mm OD / 150 mm ID), the valve and microfluidic chip holder (Micronit LOAC 4515-FS) were connected using NanoPort assemblies (Upchurch Scientific, flat bottom assembly F123-H with N-123-03). The microfluidic H-cell (Micronit B.V., Fig. S1B) was custom made out of borosilicate glass by wet-etching techniques (50 µm deep channels, 110 µm in/outlet diameter, 220 µm diameter x 32 mm length reaction zone with 6° merging angle). At the outlet, the extraction-side was connected via a Nanoport assembly to a Photo-diode Array (PDA) UV-vis detector (Shimadzu SPD-M20A with Semi-micro optical flow cell) and subsequently connected to a mass flow meter (Bronkhorst High-Tech B.V., µ-FLOW L01 series (L01-RZ*D-99-K-80S) with 10/32 UNF female connections) with fingertights (Upchurch Scientific, F120). The residual-side was connected via a Nanoport assembly to a mass flow meter with controller (Bronkhorst High-Tech B.V., µ-FLOW L01 series (L01V02-RZ*D-99-K-80S) with 10/32 UNF female connections). After the flow meter/regulator instruments, standard Teflon HPLC tubing (Upchurch Scientific, 1/16" OD / 200 mm ID) was used to fill-up sample vials in a gas-tight configuration.

The microfluidic cell holder was placed under an optical microscope in order to detect dust at the end of the reactor zone. The syringe pump, PDA and flow meter/regulators were controlled by their commercial software on a PC.

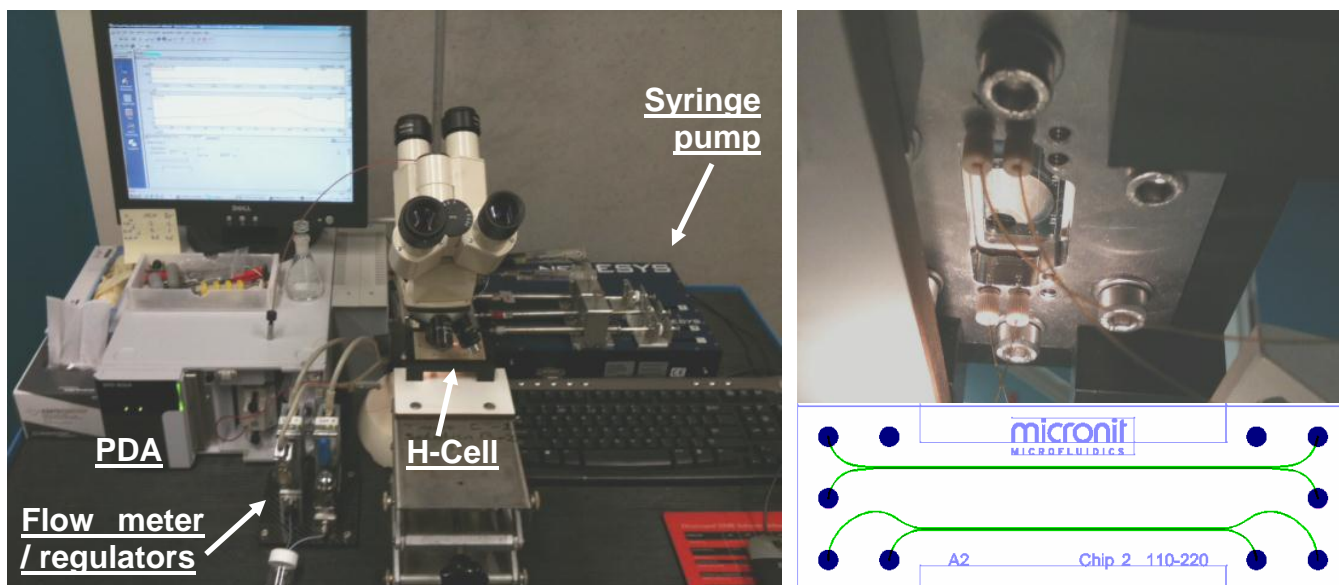


Fig. S1 (A) Overview of the microfluidic setup. (B) Chip holder containing the glass chip (outlined below) and the Nanoport assemblies to connect the fluid in/outlets with fused silica tubing.

System calibration

Prior to the measurements, the syringe(s)(pump), flow meters and PDA detector were calibrated.

Syringe pump

The linearity of the pump-syringe combinations was verified by dosing a certain amount of water in a closed vial. The diameter of the stainless steel syringes was accurately measured ($18.095 \mu\text{l}\cdot\text{mm}^{-1}$) and submitted to the software of the dosing unit (neMESYS user interface). The weight of random doses injected into the vial corresponded extremely well with the indicated volume.

Mass flow meter

The default factory calibration performed on water (linear readout until $2.0 \text{ g}\cdot\text{h}^{-1}$) was modified in the software (FlowDDE2 / FlowPlot). In the calibration procedure, this default meter readout is converted to a linear relation between the mass flow through the instrument and its indicated value *via* a 3rd-degree polynomial function. After calibration of the pump system, both meters were coupled in series and MCH was pumped through both instruments at mass flow rates between $0.1386 - 2.7720 \text{ g}\cdot\text{h}^{-1}$ (0.05 and $1.00 \mu\text{l}\cdot\text{s}^{-1}$). The corresponding mass flow fractions were obtained by dividing the introduced mass flows by $2.0 \text{ g}\cdot\text{h}^{-1}$ and plotted against the meter readout (Fig. S2A), which was obtained by averaging-out the readouts during 10 minutes acquisition. The obtained curve was fitted with a 3rd-degree polynomial and its inverse function was submitted to the software, which subsequently provided true readouts as shown by the 'x = y relation' between the mass flow rate provided by the pumps and the indicated mass flow rate of the meters (Fig. S2B).

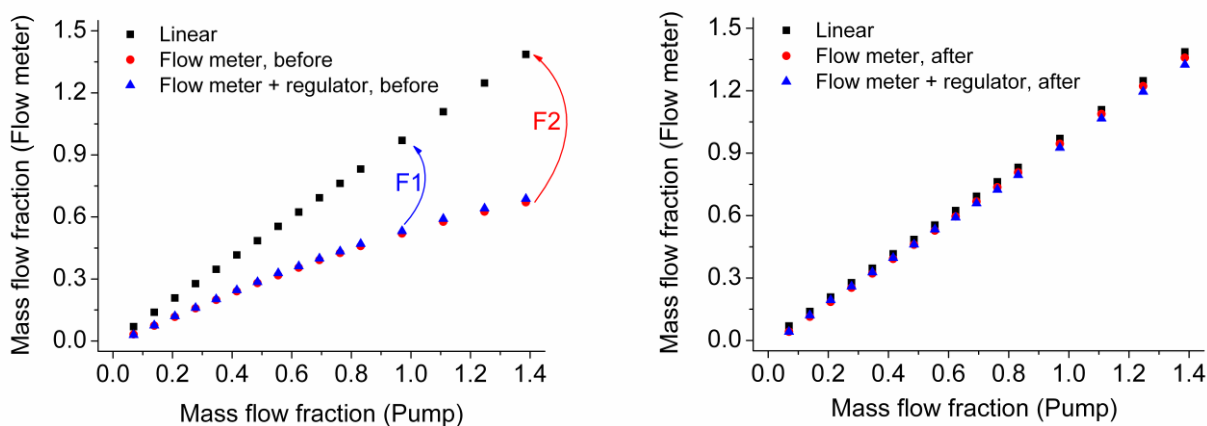


Fig. S2 True meter readouts before (A) and after (B) conversion with the 3rd-degree polynomial. $F1 = -9.006 \times 10^{-3} + 1.788x - 0.997x^2 + 1.772x^3$; $F2 = -1.137 \times 10^{-2} + 1.767x - 0.763x^2 + 1.755x^3$ with x = mass flow fraction provided by the pump.

PDA

Prior to each diffusion measurement, a calibration curve was made for pure stacks and dimers of **S-Zn** and for the monomer model compound **S-Zn-Me**. The intensity of the PDA-spectra were recorded at a flow rate of $0.5 \mu\text{l}\cdot\text{s}^{-1}$ and compared to the intensity measured on a regular UV-vis spectrometer. With the investigated flow regime, no intensity dependence on the flow rate was found.

For **S-Zn-Me** a linear calibration curve was obtained in the regular UV-vis spectrometer (Fig. S3A), whereas the linearity of the PDA detector ceased at $\sim 3 \times 10^{-6}$ M (Fig. S3A). This calibration curve was used to quantify the amount of material that diffused over, which was found in the linear part of the calibration curve for all flow rates.

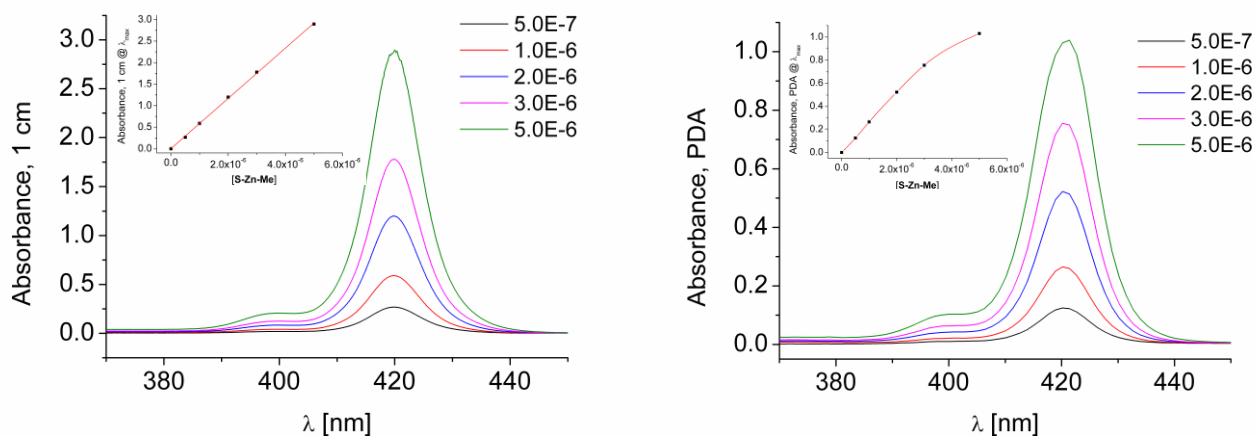


Fig. S3 UV-vis spectra of **S-Zn-Me** at different concentrations with the corresponding calibration curve (inset) measured by the UV-vis spectrometer (A) and PDA (B).

The calibration procedure of stacks was performed in the same concentration domain of $0 - 5.0 \times 10^{-6}$ M, which shows a linear relationship for both the UV-vis spectrometer (Fig. S4A) and PDA (Fig. S4B). Due to the strong association constant the linearity holds; even at low concentration enhanced monomer absorbance at $\lambda_{\text{max}} = 420$ remains absent.

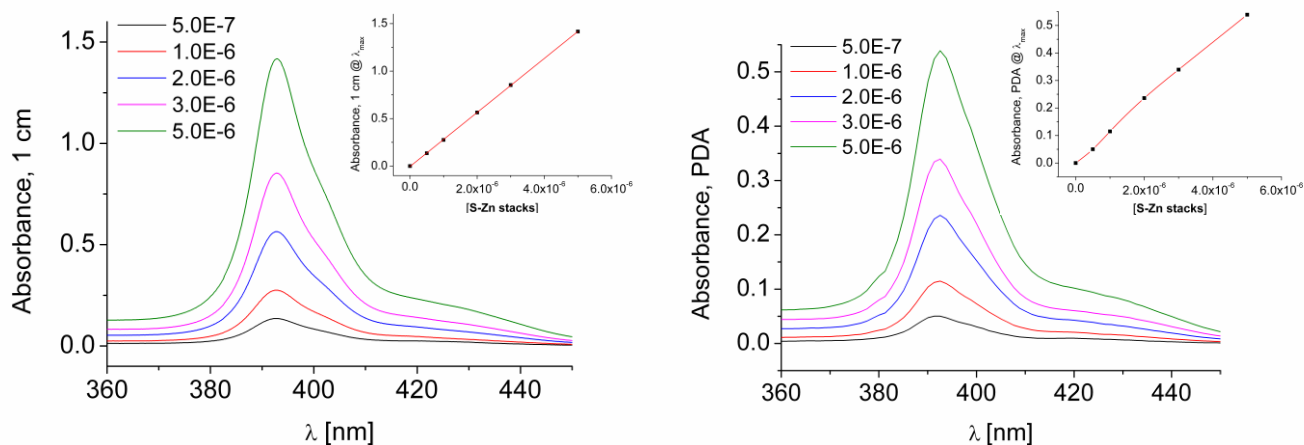


Fig. S4 UV-vis spectra of **S-Zn** stacks without pyridine at different concentrations with the corresponding calibration curve (inset) measured by the UV-vis spectrometer (A) and PDA (B).

The calibration procedure for hydrogen-bonded dimers was slightly more difficult due to the dilution-induced self-assembly. The samples at 5.0 and 2.5×10^{-6} M contained a 250 excess pyridine, yet in order to prevent dilution-induced self-assembly, more pyridine was added for the samples at 1.0×10^{-6} and 5.0×10^{-7} M. Both calibration curves show a linear relation with the dimer concentration (Fig. S5A/B).

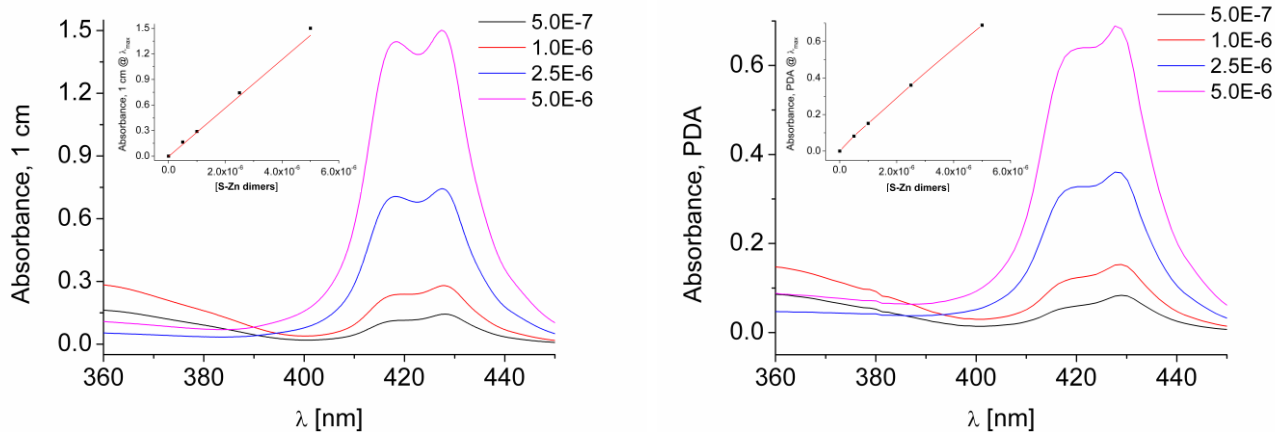


Fig. S5 UV-vis spectra of **S-Zn** dimers with pyridine at different concentrations with the corresponding calibration curve (inset) measured by the UV-vis spectrometer (A) and PDA (B).

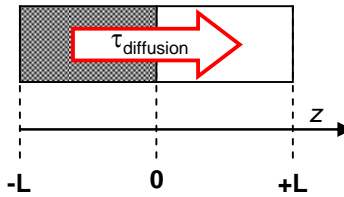
Aggregate preparation

The porphyrin stacks were prepared by dissolving solid **S-Zn** in MCH to 4.0×10^{-5} M. This stock solution was diluted to 2.0×10^{-5} M with MCH and a pyridine stock solution in MCH. Prior to the measurements, the solutions with the desired pyridine excess were aged overnight.

Diffusion studies

For the diffusion studies, 2.0×10^{-5} M porphyrin solutions (**S-Zn-Me** and **S-Zn** stacks and dimers) were pumped to one entrance of the H-cell and at equivolumetric flow rates MCH was pumped to the other entrance. Because of the hydrodynamic resistance caused by the PDA in the extraction stream and viscosity difference between both streams, a non-symmetrical split at the exit of the H-cell was observed. In order to achieve a symmetrical split at the outlets, the flow meter in the residual stream - with lower flow resistance- was equipped with a proportional-integral-derivative (PID-) controlled valve. With its tunable orifice, the valve automatically regulated the pressure drop in order to achieve an equivolumetric outflow relative to the flow meter in the extraction stream. This PID-type of control caused fluctuations, which disappeared to an acceptable level after approximately 5 minutes. Soon after reaching this steady-state condition, constant UV-vis signals were recorded by the PDA detector, which were subsequently used to determine the amount of diffused material.

Quantification was performed by correlating the recorded spectrum to the calibration curve at λ_{\max} . The corresponding concentration ($C_{\text{diffusion}}$) was divided by 1.0×10^{-5} M, which is the concentration of the fully mixed system at infinitely long diffusion time. This normalized value was plotted against the diffusion time ($\tau_{\text{diffusion}}$), and the obtained diffusion profile was fitted with a 1-dimensional unsteady-state diffusion model:

$$\frac{dC}{dt} = D \cdot \frac{d^2C}{dz^2} \Rightarrow \frac{2 \cdot C_{\text{diffusion}}}{C_{\text{in}}} = 2 \cdot \left[\frac{1}{2} - \sum_{n=0}^{n=\infty} \frac{\exp\left(-\left(n + \frac{1}{2}\right)^2 \cdot \frac{\tau_{\text{diffusion}} \cdot D \cdot \pi^2}{L^2}\right)}{\left(n + \frac{1}{2}\right)^2 \cdot \pi^2} \right]$$


After solving the Fourier series, the first three terms in the expansion were used to fit the diffusion profile. The parameters for solving: $C_{\text{in}} = 2.0 \times 10^{-5}$ M, $\tau_{\text{diffusion}} = V_{\text{reactor}} (110 \mu\text{m} \times 50 \mu\text{m} \times 32 \text{mm}) / \text{Flow rate}$, $L = 110 \mu\text{m}$ and $D = \text{diffusion coefficient} [\text{m}^2 \cdot \text{s}^{-1}]$.

The in-line UV-vis spectra of pure stacks and dimers of **S-Zn** were acquired at flow rates between 0.05 and $0.40 \mu\text{s}^{-1}$. The spectra of the stack diffusion show besides their absorbance at $\lambda_{\max} = 390 \text{ nm}$ an additional peak at $\lambda_{\max} = 420 \text{ nm}$, which indicates the presence of free monomers (Fig. S6a). The strong monomer absorbance reveals that they are present at concentrations considerably higher than the free-monomer concentration at thermodynamic equilibrium ($\sim 10^{-8}$ M).^{S1} Therefore, the acquired spectra do not represent a thermodynamically stable state, unlike the low-concentration spectra recorded for the calibration curve (Fig. S4B) that show similar stack concentrations but lack the monomer absorbance. Apparently, depolymerization occurs during the diffusion process, which is most likely due to stacks that diffuse over into a low-concentration zone.

The dimer diffusion experiment was conducted at pyridine excess of 250, which is 4-times the amount necessary to fully convert stacks into dimers at $[\text{S-Zn}] = 2.0 \times 10^{-5}$. We decided for this considerable excess to avoid dilution-induced self-assembly effects (*vide supra*), however the in-line spectra after dimer diffusion still show the presence of stacks as indicated by a shoulder at 390 nm (Fig. S6B).

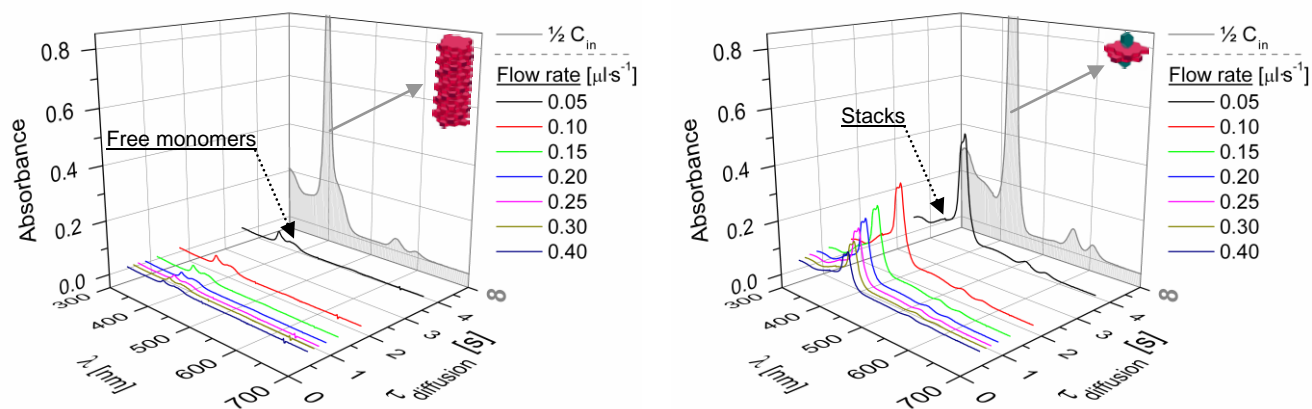


Fig. S6 In-line UV-vis spectra of **S-Zn** stacks (A) and dimers (B) acquired at different flow rates.

Validation: DOSY and DLS measurements

For validation, we performed a DOSY-NMR experiment of **S-Zn-Me** in D14-MCH at 5.0×10^{-4} M (Fig. S7A). While a translational diffusion coefficient of $\sim 8 \times 10^{-12}$ $\text{m}^2 \cdot \text{s}^{-1}$ was estimated from DLS measurements on a porphyrin sample at 6.6×10^{-5} M, the addition of pyridine causes a sharp reduction of the scattering intensity.^{S1} The dynamic measurement shows two distinctive relaxations at high and low diffusivities indicative for a fast and slow process, respectively (Fig. S7B). The latter process observed is likely due to the presence of trace amounts of dust inside the sample; a diffusion coefficient of 6×10^{-13} $\text{m}^2 \cdot \text{s}^{-1}$ is fitted from the two-exponential decay. This diffusion constant is one order of magnitude lower than observed for the **S-Zn** aggregates at similar concentration (*vide supra*), whose absence was confirmed by UV-vis and CD measurements. The fast process at low q -values indicates the presence of small objects, which are likely pyridine-capped porphyrin dimers. A diffusion coefficient of 1.3×10^{-10} $\text{m}^2 \cdot \text{s}^{-1}$ is fitted from the autocorrelation function, while a diffusion coefficient of 2.7×10^{-10} $\text{m}^2 \cdot \text{s}^{-1}$ is obtained from the microfluidic diffusion experiment.

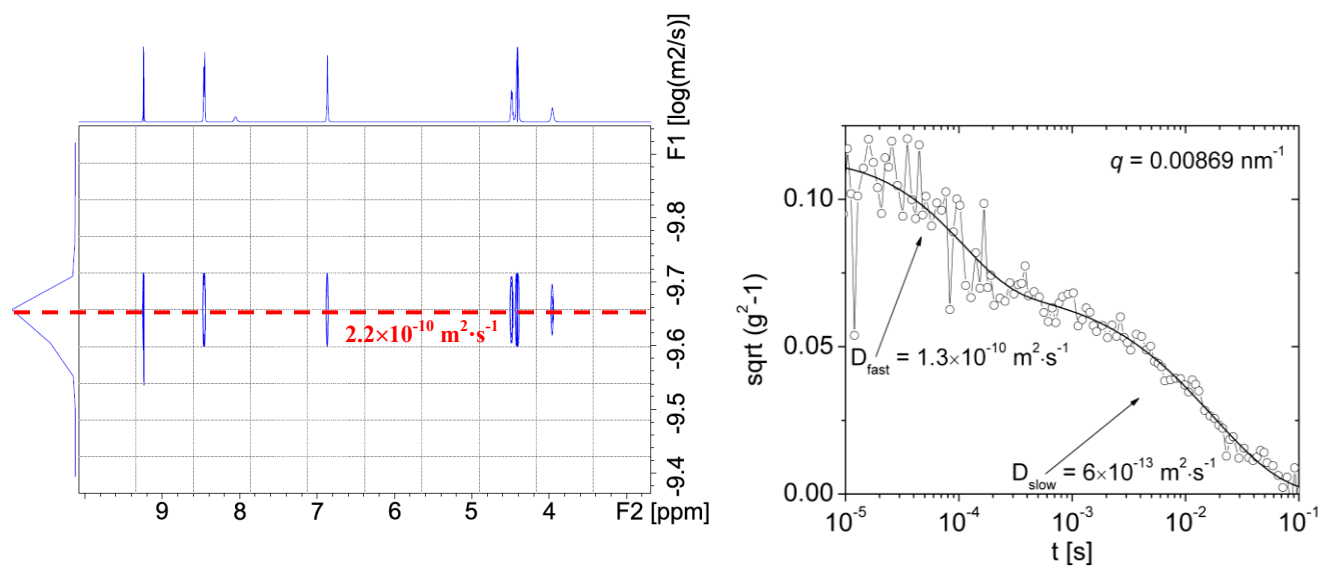


Fig. S7 (A) DOSY spectrum of **S-Zn-Me** in D14-MCH. (B) Dynamic light scattering plot at a q -value of 0.00869 nm^{-1} for **S-Zn** at 6.6×10^{-5} M in the presence of pyridine.

References

S1 Helmich, F.; Lee, C. C.; Nieuwenhuizen, M. M. L.; Gielen, J. C.; Christianen, P. C. M.; Larsen, A.; Fytas, G.; Leclère, P.; Schenning, A.; Meijer, E. W., *Angew. Chem., Int. Ed.* **2010**, *49*, 3939-3942.Ž.